JACC: BASIC TO TRANSLATIONAL SCIENCE VOL. 9, NO. 10, 2024


ORIGINAL RESEARCH - PRECLINICAL

# PCSK9 Antibodies Treatment Specifically Enhances the Macrophage-specific Reverse Cholesterol Transport Pathway in Heterozygous Familial Hypercholesterolemia

Carla Borràs, MSc,[a,b,c,*] Marina Canyelles, PhD,[a,c,*] Josefa Girona, PhD,[c,d] Daiana Ibarretxe, MD, PhD,[c,d] David Santos, BS,[a,c] Giovanna Revilla, PhD,[a,b] Vicenta Llorente-Cortes, PhD,[a,e,f] Noemí Rotllan, PhD,[a,c] Petri T. Kovanen, MD, PhD,[g] Matti Jauhiainen, PhD,[h] Miriam Lee-Rueckert, PhD,[g] Luis Masana, MD, PhD,[c,d] Francisco Arrieta, MD, PhD,[i] Javier Martínez-Botas, PhD,[j] Diego Gómez-Coronado, PhD,[j] Josep Ribalta, PhD,[c,d] Mireia Tondo, PhD,[a,c] Francisco Blanco-Vaca, MD, PhD,[a,b,c] Joan Carles Escolà-Gil, PhD[a,c]

## VISUAL ABSTRACT

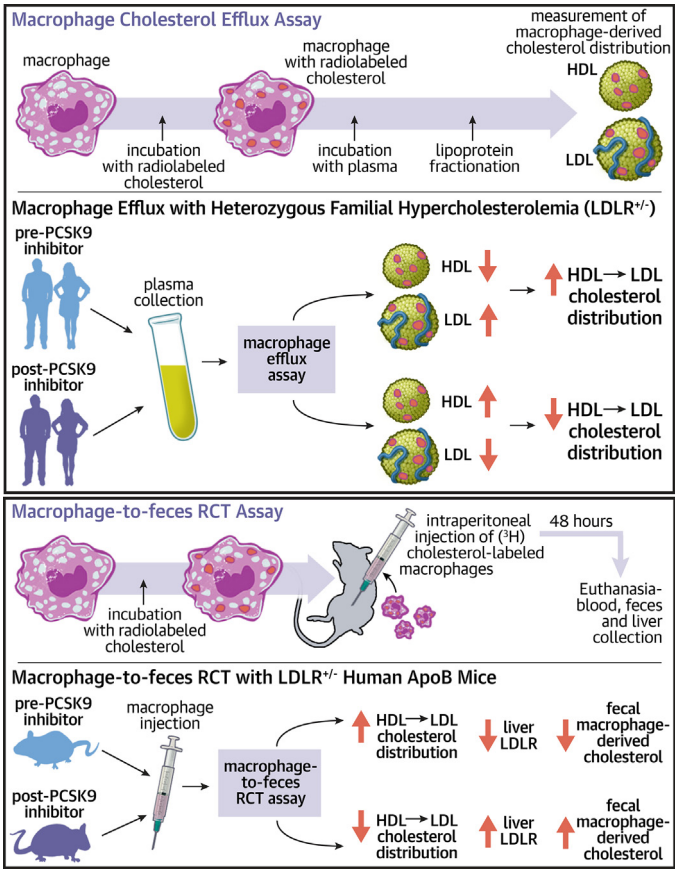


Borràs C, et al. JACC Basic Transl Sci. 2024;9(10):1195-1210.

## HIGHLIGHTS

- **PCSK9 inhibitors alter the distribution of macrophage-derived cholesterol within lipoproteins in plasma from heterozygous FH subjects during ex vivo cholesterol efflux, reducing LDL's capacity as a cholesterol acceptor while enhancing HDL's acceptor function.**
- **PCSK9 inhibition enhances the macrophage-specific reverse cholesterol transport pathway in human apoB100 transgenic mice, specifically under conditions of heterozygous LDL receptor deficiency.**
- **Anti-PCSK9 therapy facilitates the transfer of LDL-derived cholesterol to feces in heterozygous LDLR-deficient mice expressing human APOB100.**

ISSN 2452-302X https://doi.org/10.1016/j.jacbts.2024.06.008

JACC: BASIC TO TRANSLATIONAL SCIENCE VOL. 9, NO. 10, 2024
OCTOBER 2024:1195–1210

## ABBREVIATIONS AND ACRONYMS

**ABC** = ATP-binding cassette

**APO** = apolipoprotein

**CETP** = cholesteryl ester transfer protein

**DMEM** = Dulbecco's modified Eagle's medium

**HDL** = high-density lipoprotein

**HDL-C** = HDL cholesterol

**FH** = familial hypercholesterolemia

**IP** = intraperitoneal

**IV** = intravenous

**KO** = knockout

**LCAT** = lecithin:cholesterol acyltransferase

**LDL** = low density lipoprotein

**LDL-C** = low-density lipoprotein cholesterol

**LDLR** = low-density lipoprotein receptor

**LDLR+/+** = wild-type

**LDLR+/+ hAPOB100** = human APOB100 transgenic

**LDLR+/− hAPOB100** = heterozygous LDLR-deficient mice expressing hAPOB100

**LDLR−/− hAPOB100** = LDLR-KO mice expressing hAPOB100

**LPDF** = lipoprotein-depleted fraction

**LXR** = liver X receptor

**mRCT** = macrophage-specific reverse cholesterol transport

**PCSK9** = proprotein convertase subtilisin/kexin type 9

**PCSK9-mAb1** = PCSK9 antibody PL-45134

**PLTP** = phospholipid transfer protein

**RCT** = reverse cholesterol transport

**SC** = subcutaneous

**TICE** = transintestinal cholesterol excretion

**VLDL** = very-low-density lipoprotein

## SUMMARY

We investigated the potential of proprotein convertase subtilisin/kexin type 9 (PCSK9) antibodies to restore macrophage cholesterol efflux in subjects with heterozygous familial hypercholesterolemia (FH) and to enhance the macrophage-specific reverse cholesterol transport pathway in mice. Analyses of macrophage-derived cholesterol distribution of plasma from FH patients revealed that low-density lipoprotein (LDL) particles contained less, and high-density lipoprotein particles contained more radiolabeled cholesterol after treatment with either PCSK9 inhibitor. PCSK9 antibodies facilitated the transfer of macrophage-derived cholesterol and LDL-derived cholesterol to feces exclusively in heterozygous LDL receptor-deficient mice expressing human APOB100. PCSK9 inhibitors act as positive regulators of the macrophage-specific reverse cholesterol transport pathway in individuals with heterozygous FH. (JACC Basic Transl Sci. 2024;9:1195–1210) 

Familial hypercholesterolemia (FH) is a common autosomal codominant disease characterized by elevated plasma low-density lipoprotein cholesterol (LDL-C) levels and a high risk of coronary heart disease.[1] Heterozygous FH is the most usual form of the disorder, affecting approximately 1 in 300 in the general population.[2] Most FH cases are caused by loss-of-function mutations in the LDL receptor (*LDLR*) gene, but mutations in the proprotein convertase subtilisin/kexin type 9 (*PCSK9*) gene present a similar FH phenotype.[3]

Cellular cholesterol efflux, the initial step in the reverse cholesterol transport (RCT) pathway, is mediated by high-density lipoproteins (HDLs).[4] Unesterified cholesterol export from macrophages to extracellularly located HDL particles is mediated by different pathways including aqueous diffusion, receptor-facilitated diffusion by scavenger receptor class B type 1 (SR-BI) and active pathways mediated by the ATP-binding cassette (ABC) transporters A1 and G1.[4] The capacity of HDL to promote macrophage cholesterol efflux through ABCA1 has been linked to atherosclerotic cardiovascular disease, independently of HDL cholesterol (HDL-C) levels.[5,6] Several reports provide compelling evidence that an altered HDL metabolism and remodeling underlies a defective macrophage cholesterol efflux capacity of HDL in subjects with FH[7] and this is closely linked with an increased risk of atherosclerotic cardiovascular disease.[8,9] Our previous findings indicated higher lipid transfer protein activities (cholesteryl ester transfer protein [CETP] and phospholipid transfer protein [PLTP]) and lower lecithin:cholesterol acyltransferase (LCAT) activities in untreated heterozygous subjects with FH compared with normolipidemic patients, resulting in defective HDL maturation.[10] These changes correlated with impaired FH plasma and HDL fractions' ability to induce cholesterol efflux from cultured macrophages.[10,11]

From the [a]Institut de Recerca Sant Pau (IR SANT PAU), Barcelona, Spain; [b]Departament de Bioquímica i Biologia Molecular, Universitat Autònoma de Barcelona, Barcelona, Spain; [c]CIBER de Diabetes y Enfermedades Metabólicas Asociadas, CIBERDEM, Madrid, Spain; [d]Vascular Medicine and Metabolism Unit, Research Unit on Lipids and Atherosclerosis, Sant Joan University Hospital, Rovira i Virgili University, IISPV, Reus, Spain; [e]Institute of Biomedical Research of Barcelona (IIBB)-Spanish National Research Council (CSIC), Barcelona, Spain; [f]Centro de Investigación Biomédica en Red Enfermedades Cardiovasculares (CIBERCV), Instituto de Salud Carlos III, Madrid, Spain; [g]Wihuri Research Institute, Helsinki, Finland; [h]Minerva Foundation Institute for Medical Research and Finnish Institute for Health and Welfare, Department of Public Health and Welfare, Biomedicum, Helsinki, Finland; [i]Servicio de Endocrinología y Nutrición, Hospital Universitario Ramón y Cajal, IRYCIS, Madrid, Spain; and the [j]Servicio de Bioquímica-Investigación, Hospital Universitario Ramón y Cajal, IRYCIS, Madrid, Spain. *Ms Borràs, and Dr Canyelles, contributed equally to this work.

The authors attest they are in compliance with human studies committees and animal welfare regulations of the authors' institutions and Food and Drug Administration guidelines, including patient consent where appropriate. For more information, visit the Author Center.

Manuscript received February 22, 2024; revised manuscript received June 18, 2024, accepted June 18, 2024.

An early report established that a significant portion of unesterified cholesterol released from fibroblasts during efflux to HDL was rapidly transferred to LDL, becoming a major intermediate acceptor of cellular-derived cholesterol.[12] Consistent with these findings, our investigations revealed that LDL served as a reservoir for cholesterol released from macrophages via HDL in both in vitro and ex vivo experimental settings.[11] Furthermore, cholesterol derived from labeled macrophages was promptly transferred to plasma in vivo, predominantly associating with circulating LDL in Ldlr-deficient mice or Pcsk9-overexpressing mice.[11] This led to a substantial impairment in the fecal excretion of macrophage-derived cholesterol in these mice, underscoring the essential role of LDLR in supporting the macrophage-specific reverse cholesterol transport (mRCT) pathway.[11] The lack of CETP activity in these hypercholesterolemic mouse models highlighted the presence of a CETP-independent mRCT pathway, wherein LDL mediated the transfer of unesterified cholesterol from macrophages to feces.[11]

PCSK9 binds to LDLR, directing it to lysosomes for its degradation in the liver.[13] Monoclonal PCSK9 antibodies, such as alirocumab and evolocumab, have emerged as drugs to reduce LDL-C and cardiovascular disease. Indeed, both drugs have shown significant cholesterol-lowering efficacy and a reduction in the risk of cardiovascular events in patients at high cardiovascular risk.[14,15] Both PCSK9 antibodies also caused a modest increase in circulating HDL-C and apolipoprotein (APO) A1 levels.[14,15] However, current data do not support a positive effect of monoclonal PCSK9 antibodies on both plasma and HDL-mediated cholesterol efflux capacities.[16-18]

In this study, we investigated the impact of PCSK9 inhibition therapy on restoring macrophage cholesterol efflux facilitated by heterozygous FH plasma. In addition, we examined the distribution of macrophage-derived cholesterol among FH lipoproteins and assessed the effect of PCSK9 antibodies on the mRCT rate in various mouse models of hypercholesterolemia. Our results demonstrate that PCSK9 inhibitor therapy reduces the capacity of LDL to serve as a transient macrophage-derived cholesterol plasma reservoir, whereas increases that of HDL in FH subjects and enhances the mRCT in a humanized heterozygous FH mouse model.

## METHODS

**HUMAN SAMPLES.** Plasma samples were collected from adult patients with FH before and after treatment with a PCSK9 inhibitor from 2 Spanish hospitals: Hospital Universitario Ramón y Cajal and Hospital Universitario Sant Joan de Reus. The study was conducted in accordance with the ethical principles outlined in the Declaration of Helsinki and was approved by the Ethical and Clinical Investigation Committee of the 2 Spanish hospitals (protocol codes C-GEN-007 and 039/2019). All patients were clinically classified as having probable or definite FH based on the Dutch Lipid Clinic Network Score. All subjects initiated PCSK9 inhibition therapy because LDL-C levels were beyond the recommended targets despite high-intensity statins plus ezetimibe, following the current guidelines for dyslipidemia treatment by the European Atherosclerosis Society and the European Society of Cardiology.[19] These patients were treated with evolocumab or alirocumab at the doses of 140 or 75 mg, respectively, every 14 days. The average duration between baseline and post-treatment samples was 49 days for evolocumab and 60 days for alirocumab.

**MICE AND DIET.** The experimental procedures were reviewed and approved by the Institutional Animal Care and Use Committee of the Sant Pau Research Institute and authorized by the Animal Experimental Committee of the local government authority (Generalitat de Catalunya, authorization no. 10626) in accordance with the Spanish Law (RD 53/2013) and European Directive 2010/63/EU. Procedures were conducted at the Animal Experimentation Service, ISO 9001:2015 certified. Wild-type mice (LDLR+/+) and total Ldlr-deficient (KO) mice on the C57BL/6 background were purchased from Jackson Laboratories (#000664 and #002207, respectively). Human APOB100 transgenic (LDLR+/+ hAPOB100) mice on the C57BL/6 background were purchased from Taconic Biosciences (#1004-M). Ldlr-KO mice were crossbred with hAPOB100 Tg mice to generate heterozygous Ldlr-deficient mice expressing hAPOB100 (LDLR+/− hAPOB100). LDLR+/− hAPOB100 were crossbred with Ldlr-KO to generate the Ldlr-KO mice expressing hAPOB100 (LDLR−/− hAPOB100). Mice were genotyped by polymerase chain reaction (PCR) analysis on tail tip genomic DNA using primers for *Ldlr* (Jackson Laboratories), whereas hAPOB100 transgenics were detected by assessing the serum hAPOB100 levels with an immunoturbidimetric assay adapted for a COBAS 6000/501c autoanalyzer (Roche Diagnostic). Mice were kept in a temperature-controlled (22 °C) room with a 12-hour light/dark cycle, and food and water were provided ad libitum. We used 8- to 10-week-old male and female mice fed with a Western-type diet (TD.88137, Harlan Teklad, containing 21% fat and 0.2% cholesterol) for 4 weeks. The

PCSK9 recombinant antibody PL-45134 (PCSK9-mAb1) was provided by Amgen. We conducted a small pilot study to investigate whether PL-45134 (10 mg/kg), administered by intraperitoneal (IP) injection or subcutaneous (SC) injection, had a similar effect on non-HDL cholesterol in LDLR+/− hAPOB100 mice. After 2 weeks of treatment, comparable outcomes were observed: 6.7 ± 0.8 mM in IP PCSK9mAb-treated mice vs 8.2 ± 0.9 mM in vehicle mice, and 5.6 ± 1.4 mM in SC PCSK9mAb-treated mice vs 7.5 ± 0.7 mM in vehicle mice. Due to its widespread use in mice and technical simplicity, mice were injected IP with 10 mg/kg of the PCSK9-mAb1 or the vehicle solution (phosphate-buffered saline) once per week for 4 weeks. PCSK9-mAb1 was reported to be an efficient antagonist of mouse PCSK9 function.[20] Given that we previously demonstrated comparable mRCT rates in both male and female mice,[21,22] we maintained an equal distribution of males and females in these experiments, except for the wild-type mice, which were exclusively male. The number of mice per group was estimated considering $\alpha = 0.05$, power = 80%, and an effect size of 6,500 counts per minute in the fecal excretion of macrophage-derived cholesterol. Throughout all experiments, we randomized subjects with the same genotype and age into groups to achieve equal sample sizes, and all animals were included in the analyses. Whenever feasible, experiments were conducted in a blinded manner concerning the origin of the specimens to reduce bias.

**LIPID AND APOLIPOPROTEIN ANALYSES.** Plasma/serum total cholesterol, triglycerides, and HDL-C were determined enzymatically, whereas hAPOA1 and hAPOB were determined using immunoturbidimetric assays adapted for COBAS 6000/501c autoanalyzer (Roche Diagnostics). LDL-C levels in human plasma were calculated using the Friedewald formula, given that all samples had triglycerides <4.5 mmol/L. In the mouse studies, HDL-C levels were determined in serum after precipitating APOB-containing lipoprotein particles with 0.44 mmol/L phosphotungstic acid (Merck) and 20 mmol/L magnesium chloride (Sigma-Aldrich). Mouse very low-density lipoprotein (VLDL) (≤1.006 g/mL), LDL (1.019-1.063 g/mL), HDL (1.063-1.210 g/mL), and the lipoprotein-depleted fraction (LPDF ≥1.210 g/mL) were isolated from the serum through sequential ultracentrifugation, using potassium bromide for density adjustment, at 100,000 g for 24 hours with an analytical fixed-angle rotor (50.3; Beckman Coulter). The cholesterol content in each lipoprotein fraction was determined using commercial kits adapted for the COBAS 6000/501c autoanalyzer.

**ENZYME ACTIVITIES.** Both human and mouse PLTP activities were measured with a commercial assay that measures the transfer of a fluorescent substrate from a donor particle in the presence of plasmas/serums (Sigma-Aldrich/Merck). A CETP activity assay kit (Sigma-Aldrich/Merck) was used to detect the human CETP-mediated transfer of a neutral fluorescent lipid from a substrate to a physiological acceptor without being affected by variations in the endogenous lipoprotein concentrations of human plasma. LCAT activities in human plasma and mouse serum were measured via a fluorometric method that evaluates phospholipase activities (Sigma-Aldrich/Merck).

**MACROPHAGE CHOLESTEROL EFFLUX.** In vitro and ex vivo cellular cholesterol efflux was evaluated using a radiochemical method with J774A1.1 mouse macrophages (ATCC TIB67), as previously described.[11] Briefly, $2 \times 10^5$ cells/well were seeded in 6-well plates and allowed to grow for 72 hours in complete Dulbecco's modified Eagle's medium (DMEM) high glucose with L-glutamine and with sodium pyruvate (Corning) supplemented with 10% fetal bovine serum (Pan Biotech) and 100 U/mL penicillin/streptomycin (Dominique Dutscher). At that time point, the macrophages were labeled with DMEM containing 1 μCi/well of [1α,2α(n)-$^3$H]cholesterol (Perkin Elmer) and 5% fetal bovine serum for 48 hours. Then, the macrophages were equilibrated overnight with 0.2% free fatty acid bovine serum albumin (Sigma-Aldrich/Merck) in DMEM and the following day, macrophages were incubated for 4 hours with the cholesterol acceptors in the medium. Given that the liver X receptor (LXR)/retinoid X receptor complex is a permissive heterodimer that can be activated by synthetic LXR ligands,[23] all experiments were also performed under experimental settings that stimulate the ABCA1/ABCG1-dependent cholesterol efflux by treating macrophages with 2 μmol/L of the LXR T0901317 compound (Cayman Chemicals) in the equilibrating overnight period. For in vitro analyses, a pool of plasmas from normolipemic individuals (2.5%, vol/vol) and mature HDL isolated by ultracentrifugation from the same pool (at density 1.063-1.210 g/mL, 25 μg/mL of APOA1) were used as acceptors. LDL was isolated by ultracentrifugation at density 1.019-1.063 g/mL and incubated with the acceptors at a range of concentrations from 0 to 25 μg/mL of APOB. For ex vivo analyses, cholesterol acceptor was plasma at 2.5% (vol/vol) and 75 μL of plasma after precipitation of apo B-containing lipoproteins (equivalent to 2.5% of plasma) with 0.44 mmol/L phosphotungstic acid and 20 mmol/L magnesium chloride (Merck). Plasma

samples were derived from FH individuals before and after treatment with the PCSK9 inhibitor. The percentage of macrophage cholesterol efflux was calculated by dividing radiolabeled cholesterol in the medium by the sum of radiolabeled cholesterol in medium and in macrophages via liquid scintillation counting at the end of the experiments. After a 4-hour incubation period, the lipoprotein fractions (VLDL, LDL, HDL) and LPDF of the plasmas were also isolated from the medium via sequential ultracentrifugation, and the radioactivity associated with each fraction was measured to calculate the percentages of macrophage-derived cholesterol accumulated in each fraction.

**MACROPHAGE-DERIVED CHOLESTEROL TRANSFERENCE BETWEEN HUMAN HDL AND LDL.** Cholesterol efflux to human HDL was performed as described previously. Subsequently, human LDL at various concentrations was introduced into the media containing radiolabeled [$^3$H]HDL and incubated at 37°C for different time points in the absence of macrophages. The radioactivity of each lipoprotein fraction was assessed by precipitating the APOB-containing lipoproteins, as reported previously.

**IN VIVO mRCT ASSAY.** Mouse J774A.1 macrophages were cultured in 75-cm$^2$ tissue culture flasks in DMEM-supplemented medium and incubated for 48 hours in the presence of 5 μCi/mL of [1α,2α(n)-$^3$H]cholesterol. These cells were washed, equilibrated with medium containing 0.2% bovine serum albumin, detached via scraping, resuspended in phosphate-buffered saline, and pooled before being IP injected into the mice (average of $1.7 \times 10^6$ macrophages containing $1.7 \times 10^6$ cpm per mouse; cell viability was 85%, as measured by trypan blue staining). Mice were then individually housed and stools collected over the next 48 hours. At that point, the mice were euthanized and exsanguinated with cardiac puncture, and their livers were removed. Lipoproteins were isolated from 48-hour serum as described, and [$^3$H]cholesterol radioactivity was measured in each lipoprotein fraction via liquid scintillation counting. Liver and fecal lipids were extracted with isopropyl alcohol-hexane (2:3, vol/vol) as previously described.[24] The hepatic lipid layer was collected, and [$^3$H]cholesterol was measured via liquid scintillation counting. The fecal lipid layer was also collected and evaporated, and [$^3$H]cholesterol radioactivity was measured via liquid scintillation counting. The [$^3$H]tracer detected in fecal bile acids was determined for the remaining aqueous portion of fecal material extracts. The amount of [$^3$H]tracer was expressed as a fraction of the injected dose.

**HDL AND LDL KINETICS.** Mouse LDL and HDL from each genotype were isolated by sequential ultracentrifugation as described previously. For radiolabeling of both mouse lipoproteins, 50 μCi of cholesteryl-[1,2-$^3$H(N)] oleate (Perkin Elmer) and 1.8 mg of L-α-phosphatidylcholine from egg yolk (Sigma-Aldrich) were mixed, and the solvent was evaporated under a stream of $N_2$. Two milliliters of 1.006 g/mL density solution (0.05 g/L chloramphenicol [Sigma-Aldrich], 8.75 g/L sodium chloride [Sigma-Aldrich], 0.08 g/L gentamicin [Laboratorios Normon], and 0.37 g/L EDTA [Sigma-Aldrich]) was added, and the lipids were resuspended via vortex mixing; the suspension was sonicated for 10 minutes in a bath-type sonicator. The cholesteryl-[1,2-$^3$H(N)] oleate emulsion was added to 2 mL of mouse lipoproteins (LDL or HDL) and 2 mL of non-inactivated human LPDF as a source of CETP and incubated for 18 hours in a 37°C bath. The labeled LDL and HDL were reisolated by ultracentrifugation at 1.019-1.063 g/mL and 1.063-1.210 g/mL, respectively, as reported previously, and potassium bromide was removed by gel filtration chromatography. Radiolabeled LDL and HDL electrophoretic mobilities were matched with those of non-radiolabeled circulating lipoproteins; more than 75% of the radioactive label was analyzed to be bound to LDL and HDL, respectively. Each mouse was intravenously (IV) injected with 400,000 cpm of radiolabeled LDL or HDL in 0.1 mL of 0.9% NaCl via the retro-orbital venous plexus, and individually housed in order to collect stools over the next 48 hours. Blood was collected from each mouse at 2 minutes and 2, 6, 24, and 48 hours and serum radioactivity was determined. Computer analysis was used to fit an exponential curve to each set of serum-decay data and to calculate the reciprocal area under the curve (pools/hour). At the end of the experiment, liver and fecal [$^3$H]cholesterol and the [$^3$H]tracer detected in fecal bile acids were determined as described previously.

**QUANTITATIVE REAL-TIME PCR AND WESTERN BLOT ANALYSES.** For quantitative real-time PCR analyses, total liver RNA was extracted using TRIzol LS Reagent (Invitrogen) following the manufacturer's instructions. cDNA was generated using EasyScript First-Strand cDNA Synthesis SuperMix (Transgen Biotech) and quantitative real-time PCR amplification was performed using the GoTaq(R) Probe qPCR Master Mix (Promega). Specific TaqMan probes (Applied Biosystems) were used for *Abcg5* (Mm00446241_m1), *Abcg8* (Mm00445980_m1), *Ldlr* (Mm00440169_m1), and *Rn18s* (Mm03928990_g1) was used as internal control gene. Reactions were run on a CFX96TM

Real-Time System (Bio-Rad) according to the manufacturer's instructions. Thermal cycling conditions included 10 minutes at 95 °C before the onset of the PCR cycles, which consisted of 40 cycles at 95 °C for 15 seconds and at 65 °C for 1 minute. The relative mRNA expression levels were calculated using the ΔΔCt method.

For Western blot analyses, livers were lysed in RIPA buffer (50 mM Tris-HCl, pH 7.5; 150 mM NaCl; 1% NP40; 0.5% sodium deoxycholate; 0.1% sodium dodecyl sulfate; 1 mM EDTA) supplemented with protease inhibitor cocktail (Roche Diagnostics), phenylmethylsulfonyl fluoride (PMSF) (Sigma), and sodium orthovanadate (Sigma). Lysates were centrifuged at 12,000*g* for 15 minutes at 4 °C and the supernatants were collected. Protein concentrations from the supernatants were determined using a BCA protein assay reagent kit (ThermoFisher Scientific). Afterward, the protein extracts were mixed with a 4X Laemmli loading buffer and heated at 94 °C for 4 minutes. Twenty micrograms of protein were size-separated on a 10% TGX Stain-Free precast gel (Bio-Rad) and transferred to a 0.2-μm polyvinyl difluoride membrane (Bio-Rad). The membranes were blocked with 3% dried milk in Tris-buffered saline containing 0.05% of Tween-20 (TBST buffer) for 15 minutes and incubated with the primary antibody overnight at 4°C. Anti-ABCG5 and anti-ABCG8 antibodies were kindly provided by Gregory A. Graf,[25] a dilution of 1:150 was used for both antibodies. For anti-LDLR antibody (ab52818; Abcam) a dilution of 1:200 was used. Thereafter, the membranes were washed 3 times for 10 minutes with TBST buffer and re-incubated with the corresponding immunoglobulin G horseradish peroxidase-conjugated secondary antibody for 1 hour. Finally, the membranes were washed 3 times for 10 minutes with TBST buffer and analyzed using an Immun-Star Western Chemiluminescence Kit (Bio-Rad). TGX Stain-free gels were activated for 1 minute after sodium dodecyl sulfate-electrophoresis. Images were captured using a ChemiDoc XRS Gel Documentation System (Bio-Rad) and Image Lab software (version 6.0.1, Bio-Rad). Data normalization analysis for each protein band was performed with the stain-free gel images.[26,27]

**STATISTICAL METHODS.** Continuous data are presented as the mean ± SD. The Shapiro-Wilk normality test was conducted to assess the Gaussian distribution of data. Repeated measures 2-way analysis of variance (ANOVA) followed by Šídák multiple comparison test was performed to compare macrophage cholesterol efflux with plasma and the amount of radiolabeled cholesterol in the different lipoprotein fractions before and after anti-PCSK9 treatment in ex vivo cholesterol efflux assays. A paired *t*-test was conducted to compare plasma parameters and the percentage of macrophage-derived cholesterol in LDL and HDL of FH subjects before and after anti-PCSK9 treatment. One-way ANOVA followed by a post-test for linear trend was used to compare the accumulation of radiolabeled cholesterol in LDL and HDL in in vitro assays. Two-way ANOVA followed by a Tukey's multiple comparisons test was used to compare the different incubation times for each LDL concentration in cell-free studies in vitro. Unpaired *t*-tests were used to compare the differences between mice groups receiving vehicle or PCSK9 antibody treatment. GraphPad Prism version 8.0.2 for Windows (GraphPad Software) was used to perform all statistical analyses. A $P$ value ≤0.05 was considered statistically significant.

**DATA AVAILABILITY.** The data, analytical methods, and study materials will be available to other researchers for purposes of reproducing the results or replicating the procedure on reasonable request. Source data are provided with this paper (Supplemental Dataset).

## RESULTS

### PCSK9 INHIBITORS MODIFY THE LIPOPROTEIN DISTRIBUTION OF MACROPHAGE-DERIVED CHOLESTEROL EFFLUX IN HETEROZYGOUS FH.

Clinical and lipid plasma parameters are summarized in Table 1. As expected, both evolocumab and alirocumab reduced the levels of LDL-C and hAPOB, whereas HDL-C and hAPOA1 levels were not affected. The 2 PCSK9 inhibitors did not affect the HDL-associated master remodeling lipid transfer proteins and enzymes (ie, PLTP, CETP or LCAT activities).

We initially investigated the impact of PCSK9 inhibition therapy on macrophage cholesterol efflux to whole heterozygous FH plasmas. Notably, total macrophage cholesterol efflux to FH plasmas remained unaffected by either evolocumab or alirocumab treatments (Figures 1A and 1B). Given that plasmas are a physiological mixture of cholesterol acceptors and LDL particles act as a transitory reservoir of macrophage-derived cholesterol,[11] we examined the distribution of macrophage-derived cholesterol in each lipoprotein fraction and the LPDF. Both evolocumab and alirocumab therapies resulted in a reduction of radiolabeled cholesterol associated with LDL particles (Figures 1C and 1E). Significantly, the percentage of macrophage-derived cholesterol in HDL particles increased proportionally following PCSK9 inhibition therapy (Figures 1D and 1F).

**TABLE 1 Clinical and Plasma Parameters of Heterozygous FH Patients Treated With Evolocumab or Alirocumab**

| | Evolocumab (n = 14) | | | Alirocumab (n = 6) | | |
|---|---|---|---|---|---|---|
| | Pre | Post | *P* Value | Pre | Post | *P* Value |
| Clinical parameters | | | | | | |
| Male/female | 11/3 | | – | 4/2 | | - |
| BMI, kg/m$^2$ | 28.76 ± 3.15 | | – | 28.61 ± 4.65 | | - |
| Plasma parameters | | | | | | |
| Total cholesterol, mmol/L | 5.51 ± 1.11 | 3.52 ± 1.21 | <0.001 | 6.13 ± 1.61 | 2.99 ± 1.05 | <0.001 |
| LDL cholesterol, mmol/L | 3.75 ± 1.00 | 1.75 ± 1.13 | <0.001 | 4.11 ± 1.16 | 1.21 ± 0.72 | <0.001 |
| HDL cholesterol, mmol/L | 1.21 ± 0.29 | 1.22 ± 0.29 | 0.53 | 1.15 ± 0.38 | 1.16 ± 0.37 | 0.48 |
| APOA1, g/L | 1.49 ± 0.28 | 1.57 ± 0.32 | 0.15 | 1.36 ± 0.28 | 1.48 ± 0.41 | 0.12 |
| APOB100, g/L | 1.19 ± 0.23 | 0.66 ± 0.27 | <0.001 | 1.47 ± 0.38 | 0.67 ± 0.23 | <0.01 |
| Triglycerides, mmol/L | 1.18 ± 0.41 | 1.16 ± 0.54 | 0.86 | 1.91 ± 0.49 | 1.38 ± 0.29 | <0.05 |
| PLTP activity, nmol/mL/h | 63.02 ± 24.69 | 61.83 ± 18.14 | 0.79 | 46.78 ± 23.32 | 46.03 ± 15.70 | 0.86 |
| CETP activity, nmol/mL/h | 1.26 ± 0.67 | 1.18 ± 0.64 | 0.64 | 1.49 ± 0.67 | 1.29 ± 0.33 | 0.42 |
| LCAT activity, ratio 390/470[a] | 0.68 ± 0.08 | 0.67 ± 0.06 | 0.52 | 0.80 ± 0.03 | 0.77 ± 0.04 | 0.077 |

Values are n or mean ± SD. The Shapiro-Wilk normality test was conducted to assess Gaussian distribution. Paired *t*-tests were performed for all parameters. [a]The ratio between the 390-nm emission and 470-nm emission peak in the LCAT assay indicates the rate of substrate hydrolysis by LCAT.

APO = apolipoprotein; BMI = body mass index; CETP = cholesteryl ester transfer protein; FH = familial hypercholesterolemia; HDL = high-density lipoprotein; LCAT = lecithin-cholesterol acyltransferase; LDL = low-density lipoprotein; PLTP = phospholipid transfer protein.

This reduction in radiolabeled cholesterol in LDL particles and the concurrent increase in HDL particles after PCSK9 inhibition treatments were also evident when macrophage ABCA1/ABCG1-dependent pathways were stimulated (Supplemental Figure 1). VLDL particles and LPDF contained <15% of total radiolabeled cholesterol in all experimental conditions (**Figure 1**, Supplemental Figure 1). Conversely, the ability of APOB-depleted plasmas (containing mature HDL, nascent preβ-HDL particles, and key HDL-associated remodeling factors) from heterozygous FH patients to promote macrophage cholesterol efflux, under baseline conditions or experimental settings stimulating ABCA1/ABCG1-dependent efflux pathways, was moderately upregulated only by evolocumab (Supplemental Figure 2).

To further disclose the mechanism by which PCSK9 inhibition alters the distribution of macrophage-derived cholesterol between lipoproteins, we added isolated LDL from normolipidemic plasmas at increasing concentrations to isolated HDL (**Figure 2A**) or plasma (**Figure 2B**). The mixture was then added to macrophage media to stimulate cholesterol efflux. As shown in **Figures 2A and 2B**, the presence of LDL resulted in a dose-dependent reduction of macrophage-derived cholesterol accumulation in HDL particles. Notably, decreasing the LDL/HDL protein concentration (APOB/APOA1) ratio from 0.6 to 0.2 significantly increased the retained radiolabel in HDL from 13.3% to 37.3% of total cholesterol efflux, while also leading to a reduced recovery of radioactivity in LDL (**Figure 2A**). Equivalent results were found when LDL was added to HDL or plasma and exposed to macrophages pretreated with the LXR agonist to stimulate ABCA1/ABCG1-dependent pathways (Supplemental Figure 3).

As HDL is a major acceptor of macrophage-derived unesterified cholesterol, [$^3$H]HDL was isolated from the cell culture media after the efflux period and incubated with unlabeled LDL (without cells) for up to 30 minutes (**Figure 2C**). Under these conditions, a significant dose-dependent radioactivity transfer from HDL to LDL occurred (**Figure 2C**). In addition, the quantity of labeled cholesterol in LDL increased rapidly during the incubation, reaching a maximum plateau after 10 - minutes (**Figure 2C**).

**PCSK9 INHIBITION ENHANCES MACROPHAGE-TO-FECES RCT IN HUMAN apoB100 TRANSGENIC MICE ONLY UNDER CONDITIONS OF HETEROZYGOUS LDL RECEPTOR DEFICIENCY.** We aimed to assess the effects of injecting the PCSK9-mAb1 or the vehicle every 7 days on the lipoprotein profile and the mRCT pathway in LDLR+/+ hAPOB100 mice with increased circulating levels of LDL in the presence of fully functional hepatic LDL receptor. The mice were fed with a Western-type diet for 4 weeks (see the experimental outline in **Figure 3A**). Although LDLR+/+ hAPOB100 mice had 60% of cholesterol bound to LDL, the PCSK9 inhibitor had only a modest, nonsignificant impact on both LDL-C and APOB100 levels, and it did not affect HDL-associated master remodeling lipid transfer proteins and enzymes (**Table 2**). To assess the mRCT rate in vivo, [$^3$H]cholesterol-labeled

**FIGURE 1 Anti-PCSK9 Therapies Modify the Ability of LDL and HDL to Function as Macrophage Cholesterol Acceptors Ex Vivo**

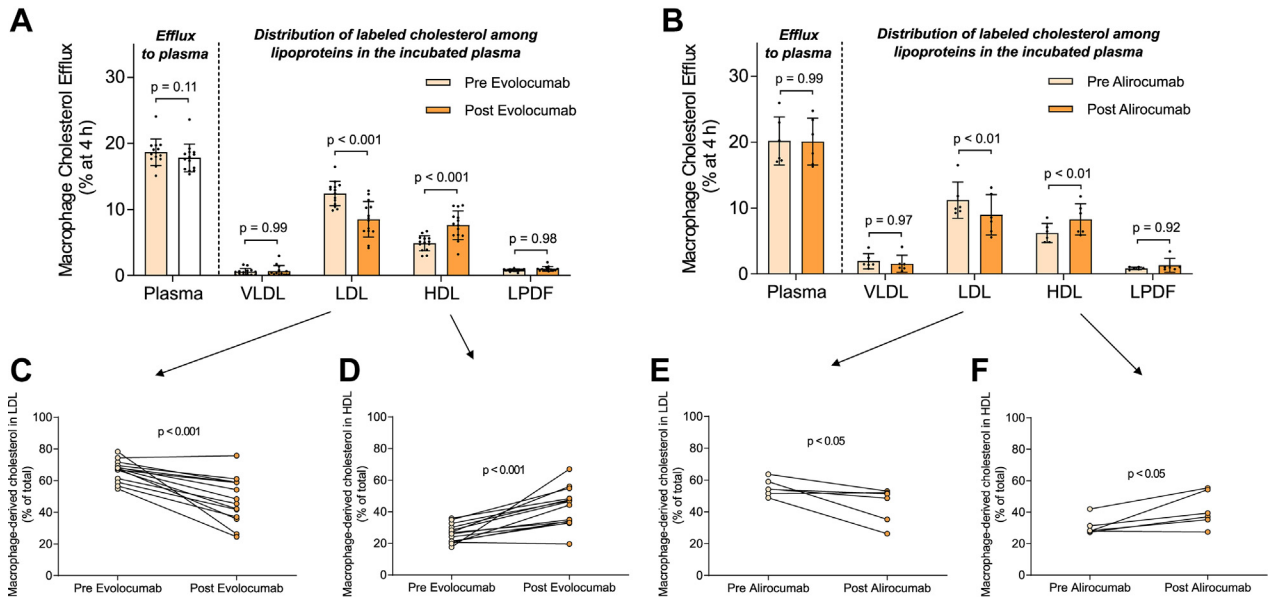


J774A.1 macrophages were exposed to media containing plasma (2.5% vol/vol) obtained from 14 heterozygous FH subjects before and after treatment with evolocumab (A) or from 6 individual heterozygous FH subjects before and after treatment with alirocumab (B) in cholesterol efflux assays. The distribution of radiolabeled cholesterol in the indicated lipoprotein fractions of the incubated plasma was determined after isolating the lipoproteins through sequential density ultracentrifugation. The percentage of the total radiolabeled cholesterol accumulated in LDL is presented as matched pairs for evolocumab (C) and alirocumab-treated (E) plasmas. The percentage of the total radiolabeled cholesterol accumulated in HDL is depicted as matched pairs for evolocumab (D) and alirocumab-treated (F) plasmas. Values in A and B are expressed as mean ± SD. A repeated measures 2-way analysis of variance followed by Šídák multiple comparison test was conducted to compare macrophage cholesterol efflux with plasma and the amount of radiolabeled cholesterol in VLDL, LDL, HDL, and LPDF. A paired *t*-test was performed to compare macrophage-derived cholesterol in LDL and HDL. FH = familial hypercholesterolemia; HDL = high-density lipoprotein; LDL = low-density lipoprotein; LPDF = lipoprotein-deleted fraction.

macrophages were injected IP into the mice, and [$^3$H]cholesterol recovery was measured in plasma, HDL, and liver at 48 hours, along with the feces collected over 48 hours (**Figure 3A**). Noteworthy, the accumulation of [$^3$H]cholesterol in LDL, HDL and liver remained unchanged after PCSK9 inhibition therapy (**Figures 3B and 3C**) and there was no modification in the fecal excretion of [$^3$H]cholesterol (**Figure 3D**).

We also evaluated whether the PCSK9 inhibitor affected the mRCT rate in LDLR+/+ mice fed a Western-type diet for 4 weeks. Approximately 75% of plasma cholesterol was bound to HDL in plasma of wild-type mice, and PCSK9 inhibition did not alter the lipoprotein profile or the HDL-associated remodeling lipid transfer proteins and enzymes (Supplemental Table 1). After injecting radiolabeled macrophages, most of the [$^3$H]cholesterol was accumulated in HDL (Supplemental Figure 4). Furthermore, PCSK9 inhibition therapy did not influence macrophage-derived cholesterol levels in serum and liver, or the overall transfer of radiolabeled cholesterol to feces (Supplemental Figure 4).

We then explored whether PCSK9 inhibition therapy could modify the mRCT rate in a mouse model of heterozygous FH, specifically in LDLR+/− hAPOB100 mice, using the same experimental outline as in **Figure 3A**. The main characteristics of plasma derived from LDLR+/− hAPOB100 mice are shown in **Table 2**. As expected, the defect in LDLR function notably increased serum levels of total cholesterol, particularly LDL-C levels. PCSK9-mAb1 significantly reduced LDL-C levels along with APOB100 levels, and these changes were not associated with alterations in PLTP or LCAT activities (**Table 2**). Notably, when [$^3$H]cholesterol-labeled macrophages were administered IP into the LDLR+/− hAPOB100 mice, the radioactivity levels in the non-HDL fraction significantly increased compared with those of LDLR+/+ and LDLR+/+ hAPOB100 mice (**Figure 3E**). Most of the radioactivity was present in LDL in LDLR+/− hAPOB100 mice (**Figure 3E**, inset). Consistent with our findings in FH patients, PCSK9-mAb1 reduced the amount of radiolabeled cholesterol in LDL particles and increased that in HDL particles (**Figure 3E**). This

**FIGURE 2** The Capacity of HDL to Serve as a Macrophage Cholesterol Acceptor Is Enhanced Through Coincubation With Low LDL Levels In Vitro

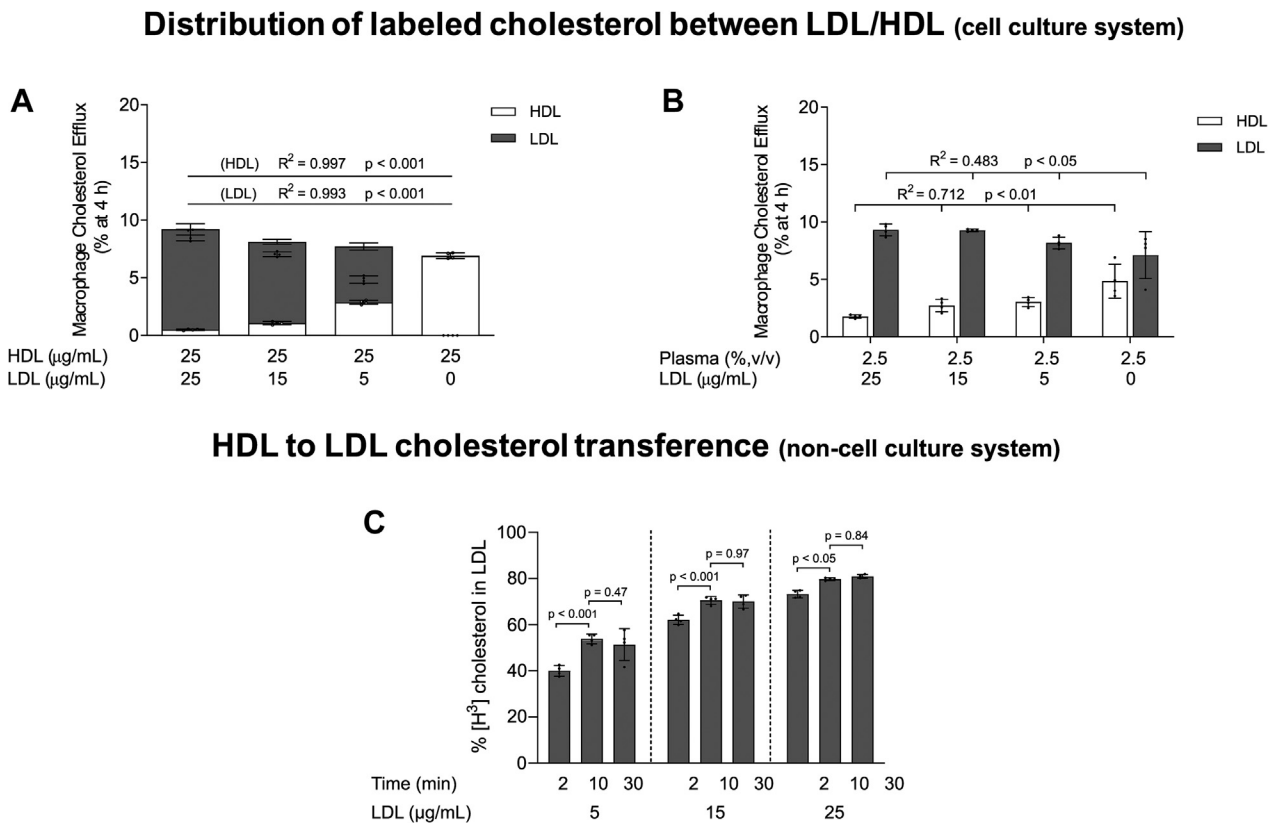


(A) In vitro cholesterol efflux from J774A.1 macrophages stimulated by HDL (25 μg/mL of APOA1) in the absence or presence of LDL added to the culture media at concentrations up to 25 μg/mL (APOB100). The distribution of labeled cholesterol between LDL and HDL was evaluated after precipitation of LDL with phosphotungstic acid-MgCl2. (B) In vitro cholesterol efflux from J774A.1 macrophages stimulated by plasma (2.5% vol/vol) in the absence or presence of LDL added to the culture media at concentrations up to 25 μg/mL (APOB100). The distribution of radiolabeled cholesterol in the lipoprotein fractions was determined after isolating the lipoproteins by sequential density ultracentrifugation. For (A) and (B), ordinary one-way ANOVA followed by a post-test for linear trend was performed to compare the accumulation of radiolabeled cholesterol in LDL and HDL. (C) Distribution of labeled cholesterol during the incubation of radiolabeled HDL isolated from cell culture media with increased concentrations of unlabeled LDL for 2, 10, and 30 minutes in a cell-free system. The amount of [$^3$H]cholesterol in HDL and LDL was determined after precipitation of LDL with phosphotungstic acid-$MgCl_2$. Values are expressed as the mean ± SD of 4 independent experiments in each condition. Two-way ANOVA followed by a Tukey's multiple comparisons test was performed to compare the different incubation times for each LDL concentration. Two-way ANOVA results were time, $P < 0.001$; LDL concentration, $P < 0.001$. ANOVA = analysis of variance; APO = apolipoprotein; other abbreviations as in Figure 1.

finding supports the notion that PCSK9 inhibitors also alter the distribution of macrophage-derived cholesterol between LDL and HDL in vivo in a mouse model of heterozygous FH. Hepatic [$^3$H]cholesterol levels were moderately lower after anti-PCSK9 treatment (Figure 3F). Importantly, the PCSK9-mAb1 enhanced the overall transfer of cholesterol from macrophages to feces in LDLR+/− hAPOB100 mice (Figure 3G).

We also investigated the impact of PCSK9 inhibition therapy on mRCT in LDLR−/− hAPOB100 mice, using the same experimental outline as in Figure 3A. This approach allowed us to test whether the full function of LDLR was required to enhance the transfer of cholesterol from blood to feces upon an anti-PCSK9 therapy. As expected, the complete lack of LDLR significantly increased serum levels of LDL-C (Supplemental Table 2). However, in the absence of LDLR, the PCSK9 inhibitor had no effect on LDL-C, APOB100, or HDL-C levels (Supplemental Table 2). Furthermore, PCSK9-mAb1 did not modify the levels of [$^3$H]cholesterol in LDL and the fecal excretion of macrophage-derived cholesterol observed in LDLR−/− hAPOB100 mice (Supplemental Figure 5).

**PCSK9 INHIBITION PROMOTES THE TRANSFER OF LDL-DERIVED CHOLESTEROL TO FECES IN HETEROZYGOUS LDLR-DEFICIENT MICE EXPRESSING HUMAN APOB100.** Considering the absence of CETP in mouse serum, we conducted kinetic experiments

**FIGURE 3 PCSK9 Inhibition Enhances the mRCT Pathway in the Human ApoB100 Transgenic Mice Only Under Conditions of Heterozygous LDL Receptor Deficiency**

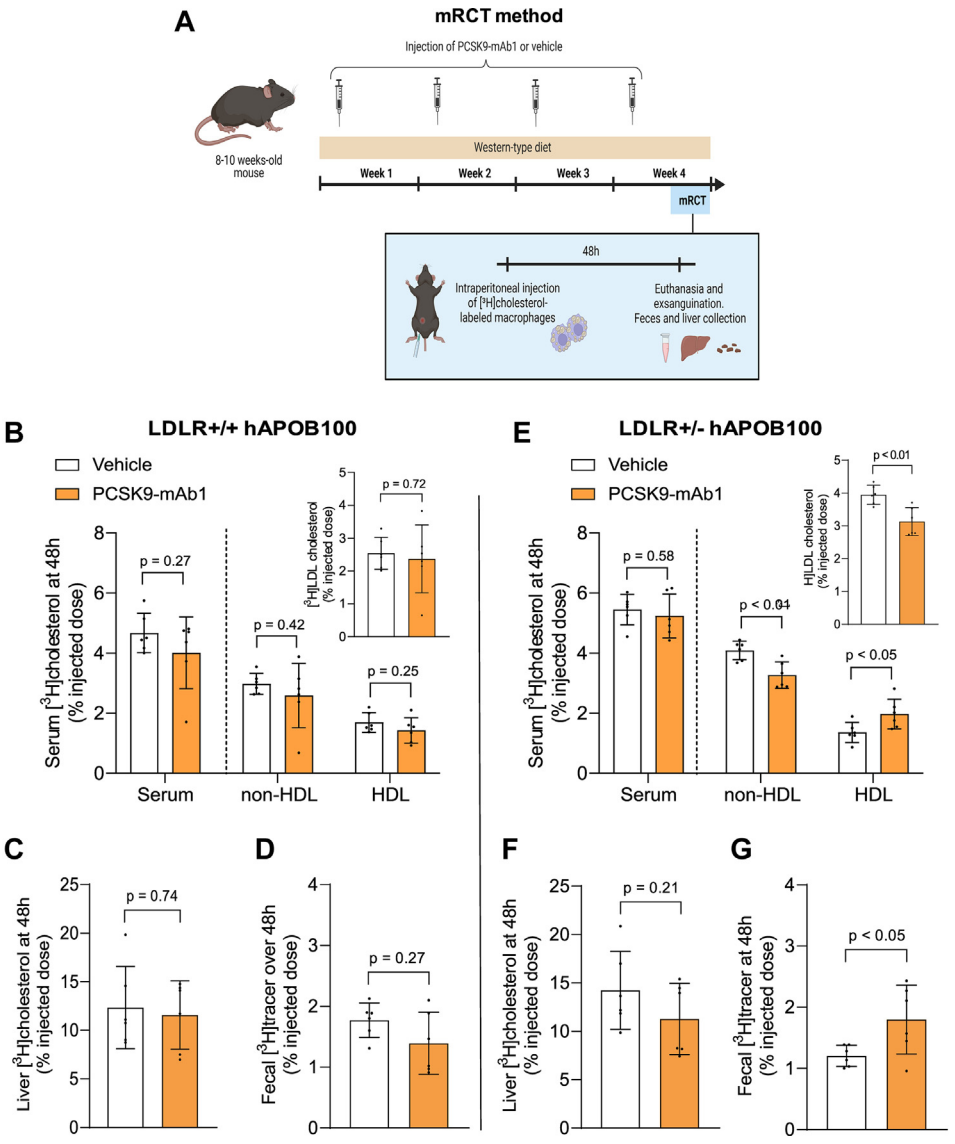


(A) Schematic representation of macrophage-to-feces reverse cholesterol transport assay. Eight- to 10-week-old mice were injected with the PCSK9 antibody PL-45134 (PCSK9-mAb1) or the vehicle every 7 days and fed a Western-type diet for 4 weeks. Forty-eight hours before the end of the experiment, mice were IP injected with J774A.1 macrophages loaded with [1α,2α(n)-$^3$H]cholesterol and housed in individual cages. At the end of the experiment, mice were euthanized and exsanguinated with cardiac puncture, their livers were removed, and individual stools were collected. (B) Serum and non-HDL [$^3$H]cholesterol at 48 hours in LDLR+/+ hAPOB100 mice treated with either PCSK9-mAb1 or the vehicle solution. Inset: [$^3$H]LDL cholesterol levels present in the non-HDL fraction. (C) Liver [$^3$H]cholesterol at 48 hours in LDLR+/+ hAPOB100 mice. Liver weights were 1.68 ± 0.30 g and 1.32 ± 0.35 g in LDLR+/+ hAPOB100 treated with the vehicle and PCSK9-mAb1-treated mice, respectively ($P = 0.084$). (D) [$^3$H]cholesterol + [$^3$H]bile acids in the feces collected over 48 hours in LDLR+/+ hAPOB100 mice. (E) Serum and non-HDL [$^3$H]cholesterol at 48 hours in LDLR+/− hAPOB100 mice treated with either PCSK9-mAb1 or the vehicle solution. Inset: [$^3$H]LDL cholesterol levels present in the non-HDL fraction. (F) Liver [$^3$H]cholesterol at 48 hours in LDLR+/− hAPOB100 mice. Liver weights were 1.56 ± 0.45 g and 1.28 ± 0.25 g in LDLR+/− hAPOB100 treated with the vehicle and PCSK9-mAb1-treated mice, respectively ($P = 0.21$). (G) [$^3$H]cholesterol + [$^3$H]bile acids in the feces collected over 48 hours in LDLR+/− hAPOB100 mice. Values are expressed as the mean ± SD of 6 individual animals per group. The amount of [$^3$H]tracer was expressed as a fraction of the injected dose. Statistics: The Shapiro-Wilk normality test was performed to test Gaussian distribution. (A) Multiple unpaired *t*-tests were performed to compare serum, [$^3$H]HDL, [$^3$H]non-HDL, and [$^3$H]LDL cholesterol levels between both groups. An unpaired *t*-test was performed to compare total liver [$^3$H]cholesterol and fecal [$^3$H]cholesterol + [$^3$H]bile acids between both groups. LDLR = low-density lipoprotein receptor; mRCT = macrophage-specific reverse cholesterol transport; PCSK9 = proprotein convertase subtilisin/kexin type 9; PCSK9-mAb1, PCSK9 antibody PL-45134; other abbreviations as in Figures 1 and 2.

**TABLE 2** Plasma and HDL Parameters in Human APOB Transgenic (LDLR+/+ hAPOB00 Tg) Mice and Heterozygous Ldlr-deficient Mice Expressing hAPOB100 (LDLR+/− hAPOB100) Treated With the PCSK9 Antibody PL-45134 (PCSK9-mAb1) or the Vehicle Solution

| | LDLR+/+ hAPOB100 | | | LDLR+/− hAPOB100 | | |
|---|---|---|---|---|---|---|
| | Vehicle (n = 6) | PCSK9-mAb1 (n = 6) | *P* Value | Vehicle (n = 6) | PCSK9-mAb1 (n = 6) | *P* Value |
| Body weight, g | 31.51 ± 7.08 | 27.44 ± 6.06 | 0.31 | 31.54 ± 4.35 | 27.23 ± 3.30 | 0.082 |
| Food intake, g/d | 2.43 ± 0.37 | 1.73 ± 0.24 | 0.14 | 2.12 ± 0.60 | 2.00 ± 0.53 | 0.72 |
| Plasma parameters | | | | | | |
| Total cholesterol, mmol/L | 7.79 ± 1.40 | 6.93 ± 2.14 | 0.43 | 14.38 ± 1.14 | 9.34 ± 1.12 | <0.001 |
| LDL cholesterol, mmol/L | 4.55 ± 1.27 | 3.83 ± 1.45 | 0.37 | 9.77 ± 1.66 | 5.58 ± 0.66 | <0.001 |
| HDL cholesterol, mmol/L | 2.98 ± 0.36 | 2.96 ± 1.25 | 0.99 | 4.36 ± 0.51 | 3.56 ± 0.74 | 0.054 |
| Triglycerides, mmol/L | 2.50 ± 0.84 | 2.06 ± 0.80 | 0.38 | 2.81 ± 0.35 | 2.67 ± 0.77 | 0.71 |
| APOB100, g/L | 1.20 ± 0.36 | 1.68 ± 1.25 | 0.39 | 2.22 ± 0.31 | 1.46 ± 0.25 | <0.001 |
| PLTP activity, nmol/mL/h | 146.94 ± 24.75 | 123.36 ± 19.76 | 0.098 | 141.06 ± 18.38 | 152.66 ± 24.86 | 0.38 |
| LCAT activity, ratio 390/470[a] | 2.96 ± 1.21 | 2.42 ± 1.33 | 0.48 | 1.52 ± 0.57 | 2.02 ± 0.91 | 0.28 |

Values are mean ± SD. The Shapiro-Wilk normality test was conducted to assess Gaussian distribution. Paired *t*-tests were performed for all parameters. [a]The ratio between the 390 nm emission and 470 nm emission peak in the LCAT assay indicates the rate of substrate hydrolysis by LCAT.

LDLR = low-density lipoprotein receptor; PCSK9 = proprotein convertase subtilisin/kexin type 9; PCSK9-mAb1 = PCSK9 antibody PL-45134; other abbreviations as in Table 1.

involving endogenous LDL and HDL to investigate the impact of circulating lipoprotein [$^3$H]cholesterol clearance on accelerated PCSK9-mAb1-mediated mRCT. Radiolabeled mouse LDL or HDL, injected IV into the mice, was monitored for tracer clearance over 48 hours, with concurrent collection of feces for radioactivity measurement (see the experimental outline in **Figure 4A**). When [$^3$H]cholesteryl oleate-radiolabeled LDL was IV injected into the LDLR+/+ hAPOB100 mice treated with the PCSK9-mAb1 or the vehicle, kinetics analyses showed that [$^3$H]LDL cholesterol decay was very fast independently of the treatment (**Figure 4B**). Furthermore, the levels of hepatic [$^3$H]cholesterol and the transfer of radioactivity to feces were not affected by PCSK9-mAb1 in the LDLR+/+ APOB100 mice (**Figures 4C and 4D**). This treatment had no impact on hepatic *Ldlr* mRNA and protein levels (Supplemental Figures 6A and 6B) and did not influence those of *Abcg5* and *Abcg8* (Supplemental Figures 6C to 6F). When [$^3$H]cholesteryl oleate-radiolabeled HDL was injected into PCSK9 antibody-treated LDLR+/+ hAPOB100 mice, [$^3$H]HDL clearance and the transfer of HDL-derived [$^3$H]cholesterol to liver and feces remained unchanged compared with the vehicle-treated control (**Figures 4E to 4G**).

As expected, kinetic analyses showed a lower decay of [$^3$H]LDL cholesterol in the LDLR+/− hAPOB100 mice (**Figure 4H**), along with reduced liver LDLR mRNA and protein levels in these mice (Supplemental Figures 6A and 6B). Importantly, radiolabeled LDL clearance was enhanced after PCSK9 inhibition therapy (**Figure 4H**). The PCSK9-mAb1 also reduced hepatic [$^3$H]cholesterol levels after the administration of radiolabeled LDL, while increasing the transfer of LDL-derived [$^3$H]cholesterol to feces in the LDLR+/− hAPOB100 mice (**Figures 4I and 4J**). These changes were associated with an upregulation of liver LDLR (Supplemental Figures 6A and 6B). PCSK9 inhibition did not modify liver mRNA or protein *Abcg5/g8* levels (Supplemental Figures 6C to 6F). Furthermore, [$^3$H]HDL clearance and the transfer of HDL-derived [$^3$H]cholesterol to the liver and feces remained unchanged in the LDLR+/− hAPOB100 mice after the treatment with PCSK9-mAb1 (**Figures 4K to 4M**).

## DISCUSSION

Significant evidence indicates that cellular-derived radiolabeled unesterified cholesterol is initially transferred to nascent preβ-HDL particles, followed by α-HDL and LDL, serving as a temporary circulatory storage pool for cell-derived unesterified cholesterol before esterification via LCAT.[12,28] The transfer of unesterified cholesterol from HDL to LDL is very fast.[12,28] Furthermore, the transfer of fibroblast-derived cholesterol from the initial acceptors to LDL is enhanced in HDL-deficient plasmas compared with those of normolipidemic plasma.[29] Cholesterol efflux capacities induced by HDL or plasma derived from untreated heterozygous FH patients are significantly impaired compared with that of normolipidemic volunteers.[10,11] Importantly, LDL also acts as a major intermediate reservoir of macrophage-derived unesterified cholesterol previously transferred to HDL during efflux process to human FH plasmas.[11] However, whether PCSK9 inhibitors may affect the capacity of LDL to serve as a transitory reservoir of macrophage-derived cholesterol is unknown. PCSK9

**FIGURE 4 PCSK9 Inhibition Promotes the Transfer of LDL-derived Cholesterol to Feces in Heterozygous Ldlr-Deficient Mice Expressing Human APOB100**

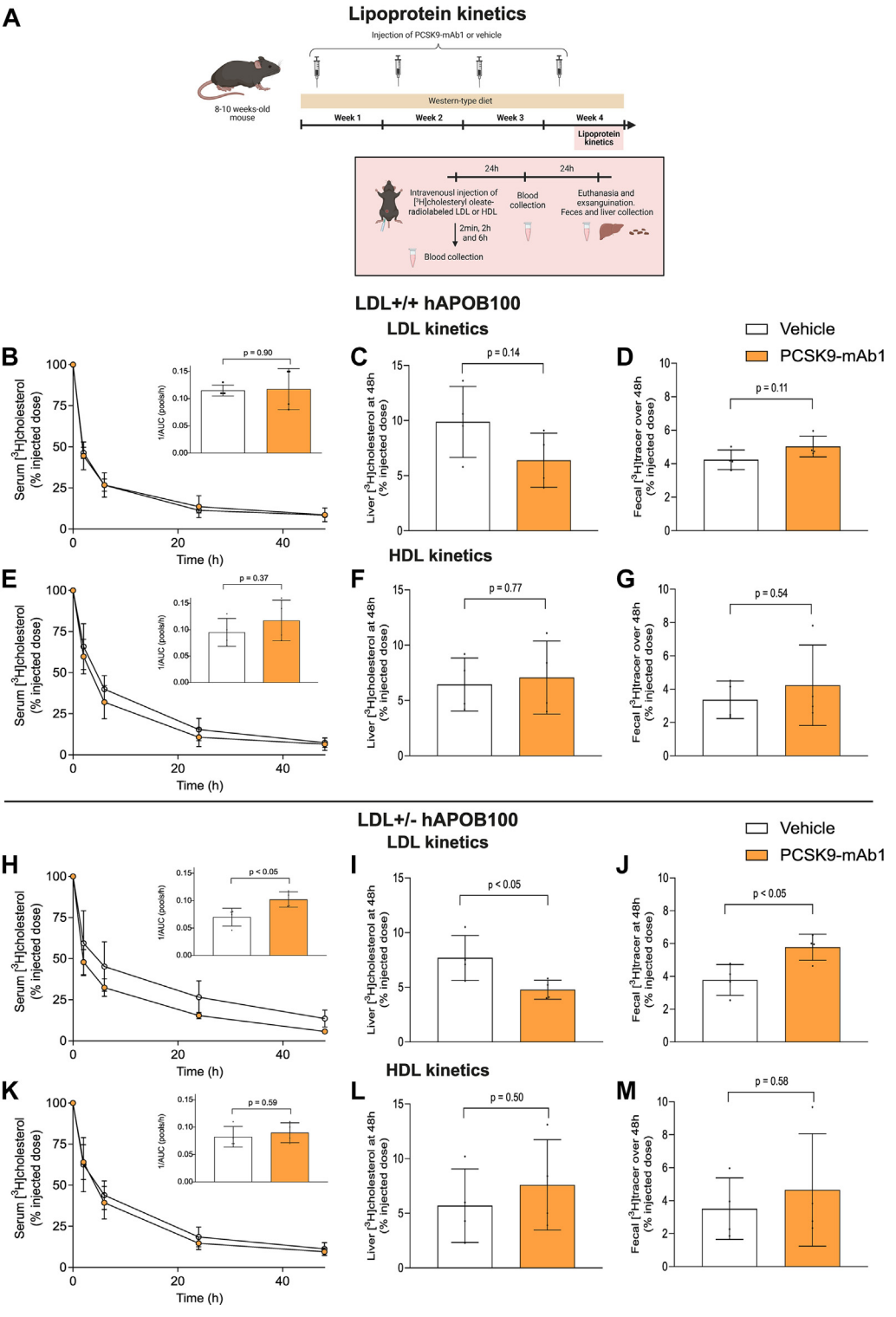


*Continued on the next page*

inhibitors appear to moderately alter the number and size of HDL particles, although the results of these studies have produced divergent outcomes[16,30,31]; furthermore, these changes seem not to have a significant impact on the ability of HDL to stimulate total macrophage cholesterol efflux.[16-18] In this study, we observed that evolocumab moderately increased the overall capacity of FH APOB-depleted plasmas, primarily reflecting the ability of HDL particles, to promote cholesterol efflux ex vivo. However, the overall capacity of FH plasmas to promote cholesterol efflux ex vivo remained unaffected by either evolocumab or alirocumab treatments. Notably, when plasmas from anti-PCSK9-treated FH subjects were fractionated, the radiolabeled cholesterol in the HDL fraction increased, whereas that bound to LDL significantly decreased. These directional changes were closely associated with the degree of plasma LDL reduction achieved by administering PCSK9-neutralizing antibodies. In line with these findings, LDL apheresis transiently reduces the ability of FH plasmas to elicit cholesterol efflux from macrophages.[32]

In our experiments using cell and non-cell culture systems, mostly devoid of master remodeling enzymes and transfer proteins, we replicated the ability of LDL to deplete macrophage-derived cholesterol from HDL particles over time in vitro. This ability was also observed by adding LDL to normolipidemic plasma. Overall, our results indicate that macrophage-derived cholesterol transfer to LDL is prevented in the circulating mixture of physiological cholesterol acceptors presented in anti-PCSK9-treated FH plasmas, resulting in the accumulation of unesterified cholesterol in HDL. This accumulation is also promoted when LDL levels are reduced under conditions that enhance the release of macrophage unesterified cholesterol via ABCA1/G1 activation.

Our previous findings have indicated that LDL also functions as a transient storage of macrophage-derived cholesterol in hypercholesterolemic plasmas in vivo.[11] Human livers produce exclusively APOB100, but a large proportion of mouse APOB is edited in the liver, producing both APOB48 and APOB100.[33] This is one of the reasons why heterozygous Ldlr-mutant rodents are resistant to diet-induced hypercholesterolemia.[34] In this study, we established an animal model of FH by crossbreeding the Ldlr-deficient mice with the hAPOB100 Tg mice. The loss of 1 copy of the *Ldlr* gene resulted in a significant increase of APOB100 and LDL-C in mice fed a Western-type diet. Consistent with our in vitro and ex vivo findings, PCSK9 antibodies reduced the accumulation of macrophage-derived cholesterol in circulating LDL-C of LDLR+/− hAPOB100 mice, whereas higher radioactivity was present in the HDL fraction. Similar to FH subjects, PCSK9 antibodies did not affect the activities of PLTP and LCAT in these FH mice. Overall, our findings indicate that PCSK9 inhibitors compromise the accumulation of macrophage-derived cholesterol in LDL particles of FH plasma independently of the main lipoprotein remodeling factors. It is noteworthy that specific cholesterol efflux originating in macrophages of the arterial intima is considered critical for preventing atherosclerosis.[35] In contrast to the peritoneal cavity, LDL particles are mainly trapped in the dense extracellular matrix by binding to

**FIGURE 4 Continued**

(A) Schematic representation of lipoprotein cholesterol kinetics assays. LDL and HDL were isolated from a pooled serum of each mouse group and incubated with [$^3$H] cholesteryl oleate preparation in the presence of CETP source (LPDF) to obtain radiolabeled LDL and HDL. Individually housed mice were treated with either PCSK9-mAb1 or the vehicle every 7 days and fed a Western-type diet for 4 weeks. Forty-eight hours before the end of the experiment, every mouse received an intravenous injection of radiolabeled autologous LDL or HDL. Blood was collected at the indicated times, and [$^3$H] counts were measured. Serum tracer decay curves were expressed as a percent of the radioactivity at the 2-minute time point after injection. At the end of the experiments, mice were euthanized, their livers were removed, and individual stools were collected. (B) In vivo clearance of [$^3$H]cholesteryl oleate-radiolabeled LDL in LDLR+/+ hAPOB100 mice treated with either the PCSK9-mAb1 or the vehicle solution. Inset: the clearance rate expressed as the reverse of the area under the curve (AUC, pools/hour). (C) Liver [$^3$H]cholesterol at 48 hours in LDLR+/+ hAPOB100 mice. (D) LDL-derived [$^3$H]cholesterol + [$^3$H]bile acids in the feces collected over 48 hours in LDLR+/+ hAPOB100 mice. (E) In vivo clearance of [$^3$H]cholesteryl oleate-radiolabeled HDL in LDLR+/+ hAPOB100 mice treated with either the PCSK9-mAb1 or the vehicle solution. Inset: the clearance rate expressed as the reverse of the area under the curve (AUC, pools/hour). (F) Liver [$^3$H]cholesterol at 48 hours in LDLR+/+ hAPOB100 mice. (G) HDL-derived [$^3$H]cholesterol + [$^3$H]bile acids in the feces collected over 48 hours in LDLR+/+ hAPOB100 mice. (H) In vivo clearance of [$^3$H]cholesteryl oleate-radiolabeled LDL in LDLR+/− hAPOB100 mice treated with either the PCSK9-mAb1 or the vehicle solution. Inset: the clearance rate expressed as the reverse of the area under the curve (AUC, pools/hour). (I) Liver [$^3$H]cholesterol at 48 hours in LDLR+/− hAPOB100 mice. (J) LDL-derived [$^3$H]cholesterol + [$^3$H]bile acids in the feces collected over 48 hours in LDLR+/− hAPOB100 mice. (K) In vivo clearance of [$^3$H]cholesteryl oleate-radiolabeled HDL in LDLR+/− hAPOB100 mice treated with either the PCSK9-mAb1 or the vehicle solution. Inset: The clearance rate expressed as the reverse of the area under the curve (AUC, pools/hour). (L) Liver [$^3$H]cholesterol at 48 hours in LDLR+/− hAPOB100 mice. (M) HDL-derived [$^3$H]cholesterol + [$^3$H]bile acids in the feces collected over 48 hours in LDLR+/− hAPOB100 mice. Values are expressed as the mean ± SD of 4 individual animals per group. The amount of [$^3$H]radiotracer was expressed as a fraction of the injected dose. Statistics: The Shapiro-Wilk normality test was performed to test Gaussian distribution. An unpaired *t*-test was performed to compare the lipoprotein clearance rates, total liver [$^3$H]cholesterol, and fecal [$^3$H] cholesterol + [$^3$H]bile acids between both groups. CETP = cholesteryl ester transfer protein; LDLR, low-density lipoprotein receptor; LDLR+/+, wild-type; LDLR+/+ hAPOB100, human APOB100 transgenic; LDLR+/− hAPOB100, heterozygous LDLR-deficient mice expressing hAPOB100; other abbreviations as in Figures 1 to 3.

proteoglycans of the arterial intima, and when modified, they are taken up by macrophages.[36] On the contrary, lymphatic vessels are critical to transport macrophage-derived cholesterol accumulated in HDL particles to the plasma during the mRCT pathway.[37] Thus, one could consider that a reduced transfer of macrophage-derived cholesterol from HDL to LDL in the intimal fluid of FH subjects treated with PCSK9 inhibitors and the consequent increase of macrophage-derived cholesterol in HDL, might stimulate the removal of cholesterol from the arterial wall.

In our previous studies, we have highlighted that LDLR functionality is crucial to sustain a CETP-independent mRCT pathway in vivo by directing the macrophage-derived cholesterol carried in LDL to the feces.[11] This current study provides additional evidence that PCSK9 antibodies enhance the clearance of LDL-derived cholesterol esters specifically in LDLR+/− hAPOB100 mice. Notably, under specific conditions, such as hepatocyte ABCA1 deletion, LDLR can modulate the selective traffic of HDL cholesterol esters.[38] However, Ldlr-KO mice did not show reduced *Abca1* expression in mice,[11] and PCSK9 antibodies show no effect on the clearance of HDL-derived cholesterol esters in LDLR+/− hAPOB100 mice. Importantly, besides the rapid decay of radioactivity in the plasma of anti-PCSK9-treated FH mice, lower levels of radioactivity remained in the liver compartment, and overall, the fecal excretion of macrophage-derived cholesterol was significantly enhanced in these mice. Liver cholesterol is ultimately secreted into the bile and the intestine in the form of unesterified cholesterol via ABCG5 and ABCG8.[39] Furthermore, dietary cholesterol plays a crucial role in the Western-type diet-mediated induction of mRCT rate by upregulating liver ABCG5 and ABCG8.[40] Given the strong upregulation of liver LDLR in the PCSK9 antibodies-treated FH mice concomitant with high expression of ABCG5/ABCG8 transporters, our results suggest that the hepatobiliary bypass of LDL is essential for explaining the enhanced cholesterol excretion mediated by PCSK9 antibodies in these mice. Consistent with these findings, overexpression of ABCG5 and ABCG8 transporters has no impact on the cholesterol balance across the liver nor does it increase the daily excretion of fecal cholesterol in livers of Ldlr-KO mice.[41] Furthermore, we also found that the PCSK9 antibody-mediated stimulus on mRCT is completely blunted in LDLR−/− hAPOB100 mice.

It is noteworthy that the increase of LDL by overexpressing hAPOB100 does not enhance the mRCT rate in mice with fully functional LDLR.[11] These findings suggest that, under these conditions, the LDLR-mediated hepatobiliary transport is saturated. Indeed, kinetics analyses reveal a rapid decay of LDL in the sera of LDLR+/+ hAPOB100 mice, and this decay is not further accelerated by the administration of PCSK9 antibodies. Furthermore, the transfer of radioactivity to feces is similar in both the control and anti-PCSK9-treated LDLR+/+ hAPOB100 mice, confirming that the LDLR pathway cannot be further modulated by PCSK9 antibodies in this mouse model.

Although an alternative transintestinal cholesterol excretion (TICE) route contributing to the removal of blood-derived unesterified cholesterol has been reported,[42] the experimental evidence from various mouse models quantifying the contribution of such an alternative TICE route to the mRCT pathway is somewhat conflicting.[43,44] TICE appears to be higher in Ldlr-KO mice[45] and conversely, it increases in Pcsk9-KO mice while being reduced after an acute injection of recombinant PCSK9 in vivo.[45] Although the effects of PCSK9 antibodies on mRCT associated with the TICE pathway are unknown, it cannot be completely ruled out that the higher mRCT observed in PCSK9 antibody-treated LDLR+/− hAPOB100 mice could involve TICE acceleration.

**STUDY LIMITATIONS.** This human study was not randomized, and the decision to administer anti-PCSK9 therapy was based on clinical judgment in a real-world clinical setting. Therefore, these findings need validation in a larger cohort of patients with FH and their association with cardiovascular risk endpoints should be explored.

In contrast to FH patients, mice do not express CETP. This enabled us to investigate the kinetics of HDL and LDL independently, as there is no transfer of esterified cholesterol between these lipoproteins. Further studies are needed to assess whether PCSK9 inhibitor therapy would enhance mRCT in the heterozygous FH mouse model expressing human CETP.

It is worth noting that recent evidence has raised doubts about the efficacy of enhancing HDL functionality with APOA1 infusions to prevent cardiovascular events.[46] Nevertheless, potential positive effects of APOA1 infusions were observed on myocardial infarction and this warrants further analysis.[47]

## CONCLUSIONS

Our study demonstrates that PCSK9 inhibitor therapy induces a shift in the distribution of macrophage-derived cholesterol to lipoproteins in FH plasma during the cholesterol efflux process. This results in a reduction of LDL's capacity to act as a macrophage-derived cholesterol acceptor and an increase in the acceptor function of HDL. Furthermore, our findings

support the positive effects of PCSK9 inhibitors on the regulation of mRCT by enhancing the LDLR-mediated hepatobiliary route in LDLR+/− hAPOB100 mice. Notably, these positive effects are absent in LDLR+/+ hAPOB100 transgenic and wild-type mice with fully functional LDLR or when LDLR is completely blocked. The present findings reveal that, in addition to their plasma LDL-cholesterol-lowering effect, PCSK9-targeted therapies may also positively impact the dynamics of cholesterol removal from the body in individuals with heterozygous FH.

## FUNDING SUPPORT AND AUTHOR DISCLOSURES

This work was partly funded by the Instituto de Salud Carlos III and FEDER "Una manera de hacer Europa" grants PI2100140 (to Dr Blanco-Vaca and Dr Tondo), PI2101523 (to Dr Llorente-Cortes), PI2300232 (to Dr Canyelles and Dr Escolà-Gil), JR22/00003 (to Dr Canyelles), by the Ministerio de Ciencia e Innovación grant RTI2018-098113-B-I00 (to Dr Gómez-Coronado), by BBVA Foundation Ayudas a Equipos de Investigación 2019 to the project "Translational Molecular Imaging for detection of Cholesterol Entrapment in the Vasculature with 68Ga-labeled LRP1-derived peptides" (to Dr Llorente-Cortes) and grant 12/C/2015 from La Fundació la Marató TV3 (to Dr Masana and Dr Blanco-Vaca); the Jane and Aatos Erkko Foundation (to Dr Jauhiainen), and the Finnish Foundation for Cardiovascular Research (to Dr Jauhiainen). Ms Borràs was funded with a Formación de Profesorado Universitario grant FPU20/07440 from the Ministerio de Universidades. Dr Rotllan was funded by Agencia Estatal de Investigación (AEI/10.13039/501100011033) within the Subprograma Ramón y Cajal (RYC-201722879). CIBERDEM and CIBERCV are Instituto de Salud Carlos III projects. All authors have reported that they have no relationships relevant to the contents of this paper to disclose.

**ADDRESS FOR CORRESPONDENCE:** Dr Joan Carles Escolà-Gil or Dr Francisco Blanco-Vaca, Institut d'Investigacions Biomèdiques (IIB) Sant Pau, C/ Sant Quintí 77, 08041 Barcelona, Spain. E-mail: jescola@santpau.cat OR fblancova@santpau.cat.

## PERSPECTIVES

**COMPETENCY IN MEDICAL KNOWLEDGE:** Heterozygous FH is associated with dysfunctional mRCT, attributed to decreased levels of HDL and impaired HDL remodeling. PCSK9 inhibitor therapy increases the capacity of HDL to act as a transient reservoir for macrophage-derived cholesterol in heterozygous FH patients and promotes mRCT in a humanized heterozygous FH mouse model.

**TRANSLATIONAL OUTLOOK:** Our results underscore the multifaceted effects of PCSK9 inhibitor therapy, not only in reducing LDL cholesterol, but also in modulating macrophage cholesterol efflux and promoting the atheroprotective mRCT pathway, particularly in the context of heterozygous FH. Future research should analyze the effects of PCSK9 inhibitors on macrophage cholesterol efflux to plasma and the distribution of macrophage-derived cholesterol among lipoproteins in other forms of hypercholesterolemia and their association with cardiovascular risk endpoints.

## REFERENCES

**1.** Nordestgaard BG, Chapman MJ, Humphries SE, et al. Familial hypercholesterolaemia is underdiagnosed and undertreated in the general population: guidance for clinicians to prevent coronary heart disease: consensus statement of the European Atherosclerosis Society. *Eur Heart J*. 2013;34:3478–3490a.

**2.** Hu P, Dharmayat KI, Stevens CAT, et al. Prevalence of familial hypercholesterolemia among the general population and patients with atherosclerotic cardiovascular disease: a systematic review and meta-analysis. *Circulation*. 2020;141:1742–1759.

**3.** Sniderman AD, Tsimikas S, Fazio S. The severe hypercholesterolemia phenotype: clinical diagnosis, management, and emerging therapies. *J Am Coll Cardiol*. 2014;63:1935–1947.

**4.** Phillips MC. Molecular mechanisms of cellular cholesterol efflux. *J Biol Chem*. 2014;289:24020–24029.

**5.** Rohatgi A, Khera A, Berry JD, et al. HDL cholesterol efflux capacity and incident cardiovascular events. *N Engl J Med*. 2014;371:2383–2393.

**6.** Saleheen D, Scott R, Javad S, et al. Association of HDL cholesterol efflux capacity with incident coronary heart disease events: a prospective case-control study. *Lancet Diabetes Endocrinol*. 2015;3:507–513.

**7.** Escolà-Gil JC, Rotllan N, Julve J, Blanco-Vaca F. Reverse cholesterol transport dysfunction is a feature of familial hypercholesterolemia. *Curr Atheroscler Rep*. 2021;23:29.

**8.** Ogura M, Hori M, Harada-Shiba M. Association between cholesterol efflux capacity and atherosclerotic cardiovascular disease in patients with familial hypercholesterolemia. *Arterioscler Thromb Vasc Biol*. 2016;36:181–188.

**9.** Ganjali S, Hosseini S, Rizzo M, Kontush A, Sahebkar A. Capacity of HDL to efflux cellular cholesterol from lipid-loaded macrophages is reduced in patients with familial hypercholesterolemia. *Metabolites*. 2023;13:197.

**10.** Cedo L, Plana N, Metso J, et al. Altered HDL remodeling and functionality in familial hypercholesterolemia. *J Am Coll Cardiol*. 2018;71:466–468.

**11.** Cedo L, Metso J, Santos D, et al. LDL receptor regulates the reverse transport of macrophage-derived unesterified cholesterol via concerted action of the HDL-LDL axis: insight from mouse models. *Circ Res*. 2020;127:778–792.

**12.** Huang Y, von Eckardstein A, Assmann G. Cell-derived unesterified cholesterol cycles between different HDLs and LDL for its effective esterification in plasma. *Arterioscler Thromb*. 1993;13:445–458.

**13.** Horton JD, Cohen JC, Hobbs HH. Molecular biology of PCSK9: its role in LDL metabolism. *Trends Biochem Sci*. 2007;32:71–77.

**14.** Robinson JG, Farnier M, Krempf M, et al. Efficacy and safety of alirocumab in reducing lipids and cardiovascular events. *N Engl J Med*. 2015;372:1489–1499.

**15.** Sabatine MS, Giugliano RP, Keech AC, et al. Evolocumab and clinical outcomes in patients with cardiovascular disease. *N Engl J Med*. 2017;376:1713–1722.

**16.** Lappegard KT, Kjellmo CA, Ljunggren S, et al. Lipoprotein apheresis affects lipoprotein particle subclasses more efficiently compared to the PCSK9 inhibitor evolocumab, a pilot study. *Transfus Apher Sci*. 2018;57:91–96.

**17.** Ying Q, Ronca A, Chan DC, Pang J, Favari E, Watts GF. Effect of a PCSK9 inhibitor and a statin on cholesterol efflux capacity: a limitation of current cholesterol-lowering treatments? *Eur J Clin Invest*. 2022;52:e13766.

**18.** Palumbo M, Giammanco A, Purrello F, et al. Effects of PCSK9 inhibitors on HDL cholesterol efflux and serum cholesterol loading capacity in familial hypercholesterolemia subjects: a multi-lipid-center real-world evaluation. *Front Mol Biosci*. 2022;9:925587.

**19.** Mach F, Baigent C, Catapano AL, et al. 2019 ESC/EAS guidelines for the management of dyslipidaemias: lipid modification to reduce cardiovascular risk. *Eur Heart J*. 2020;41:111–188.

**20.** Chan JC, Piper DE, Cao Q, et al. A proprotein convertase subtilisin/kexin type 9 neutralizing antibody reduces serum cholesterol in mice and nonhuman primates. *Proc Natl Acad Sci U S A*. 2009;106:9820–9825.

**21.** Calpe-Berdiel L, Rotllan N, Fievet C, Roig R, Blanco-Vaca F, Escola-Gil JC. Liver X receptor-mediated activation of reverse cholesterol transport from macrophages to feces in vivo requires ABCG5/G8. *J Lipid Res*. 2008;49:1904–1911.

**22.** Rotllan N, Calpe-Berdiel L, Guillaumet-Adkins A, Suren-Castillo S, Blanco-Vaca F, Escola-Gil JC. CETP activity variation in mice does not affect two major HDL antiatherogenic properties: macrophage-specific reverse cholesterol transport and LDL antioxidant protection. *Atherosclerosis*. 2008;196:505–513.

**23.** Willy PJ, Mangelsdorf DJ. Unique requirements for retinoid-dependent transcriptional activation by the orphan receptor LXR. *Genes Dev*. 1997;11:289–298.

**24.** Escola-Gil JC, Lee-Rueckert M, Santos D, Cedo L, Blanco-Vaca F, Julve J. Quantification of in vitro macrophage cholesterol efflux and in vivo macrophage-specific reverse cholesterol transport. *Methods Mol Biol*. 2015;1339:211–233.

**25.** Wang Y, Su K, Sabeva NS, et al. GRP78 rescues the ABCG5 ABCG8 sterol transporter in db/db mice. *Metabolism*. 2015;64:1435–1443.

**26.** Taylor SC, Posch A. The design of a quantitative western blot experiment. *Biomed Res Int*. 2014;2014:361590.

**27.** Neris RLS, Dobles AMC, Gomes AV. Western blotting using in-gel protein labeling as a normalization control: advantages of stain-free technology. *Methods Mol Biol*. 2021;2261:443–456.

**28.** Xu B, Gillard BK, Gotto AM Jr, Rosales C, Pownall HJ. ABCA1-derived nascent high-density lipoprotein-apolipoprotein AI and lipids metabolically segregate. *Arterioscler Thromb Vasc Biol*. 2017;37:2260–2270.

**29.** von Eckardstein A, Huang Y, Wu S, Funke H, Noseda G, Assmann G. Reverse cholesterol transport in plasma of patients with different forms of familial HDL deficiency. *Arterioscler Thromb Vasc Biol*. 1995;15:691–703.

**30.** Koren MJ, Kereiakes D, Pourfarzib R, et al. Effect of PCSK9 inhibition by alirocumab on lipoprotein particle concentrations determined by nuclear magnetic resonance spectroscopy. *J Am Heart Assoc*. 2015;4:e002224.

**31.** Rehues P, Girona J, Guardiola M, et al. PCSK9 inhibitors have apolipoprotein C-III-related anti-inflammatory activity, assessed by 1H-NMR glycoprotein profile in subjects at high or very high cardiovascular risk. *Int J Mol Sci*. 2023;24:2319.

**32.** Orsoni A, Villard EF, Bruckert E, et al. Impact of LDL apheresis on atheroprotective reverse cholesterol transport pathway in familial hypercholesterolemia. *J Lipid Res*. 2012;53:767–775.

**33.** Greeve J, Altkemper I, Dieterich JH, Greten H, Windler E. Apolipoprotein B mRNA editing in 12 different mammalian species: hepatic expression is reflected in low concentrations of apoB-containing plasma lipoproteins. *J Lipid Res*. 1993;34:1367–1383.

**34.** Ishibashi S, Brown MS, Goldstein JL, Gerard RD, Hammer RE, Herz J. Hypercholesterolemia in low density lipoprotein receptor knockout mice and its reversal by adenovirus-mediated gene delivery. *J Clin Invest*. 1993;92:883–893.

**35.** Lee-Rueckert M, Escola-Gil JC, Kovanen PT. HDL functionality in reverse cholesterol transport-Challenges in translating data emerging from mouse models to human disease. *Biochim Biophys Acta*. 2016;1861:566–583.

**36.** Boren J, Chapman MJ, Krauss RM, et al. Low-density lipoproteins cause atherosclerotic cardiovascular disease: pathophysiological, genetic, and therapeutic insights: a consensus statement from the European Atherosclerosis Society Consensus Panel. *Eur Heart J*. 2020;41:2313–2330.

**37.** Martel C, Li W, Fulp B, et al. Lymphatic vasculature mediates macrophage reverse cholesterol transport in mice. *J Clin Invest*. 2013;123:1571–1579.

**38.** Bashore AC, Liu M, Key CC, et al. Targeted deletion of hepatocyte Abca1 increases plasma HDL (high-density lipoprotein) reverse cholesterol transport via the LDL (low-density lipoprotein) receptor. *Arterioscler Thromb Vasc Biol*. 2019;39:1747–1761.

**39.** Graf GA, Yu L, Li WP, et al. ABCG5 and ABCG8 are obligate heterodimers for protein trafficking and biliary cholesterol excretion. *J Biol Chem*. 2003;278:48275–48282.

**40.** Escola-Gil JC, Llaverias G, Julve J, Jauhiainen M, Mendez-Gonzalez J, Blanco-Vaca F. The cholesterol content of Western diets plays a major role in the paradoxical increase in high-density lipoprotein cholesterol and upregulates the macrophage reverse cholesterol transport pathway. *Arterioscler Thromb Vasc Biol*. 2011;31:2493–2499.

**41.** Wu JE, Basso F, Shamburek RD, et al. Hepatic ABCG5 and ABCG8 overexpression increases hepatobiliary sterol transport but does not alter aortic atherosclerosis in transgenic mice. *J Biol Chem*. 2004;279:22913–22925.

**42.** Grefhorst A, Verkade HJ, Groen AK. The TICE pathway: mechanisms and lipid-lowering therapies. *Methodist Debakey Cardiovasc J*. 2019;15:70–76.

**43.** Temel RE, Sawyer JK, Yu L, et al. Biliary sterol secretion is not required for macrophage reverse cholesterol transport. *Cell Metab*. 2010;12:96–102.

**44.** Nijstad N, Gautier T, Briand F, Rader DJ, Tietge UJ. Biliary sterol secretion is required for functional in vivo reverse cholesterol transport in mice. *Gastroenterology*. 2011;140:1043–1051.

**45.** Le May C, Berger JM, Lespine A, et al. Transintestinal cholesterol excretion is an active metabolic process modulated by PCSK9 and statin involving ABCB1. *Arterioscler Thromb Vasc Biol*. 2013;33:1484–1493.

**46.** Gibson CM, Duffy D, Korjian S, et al. Apolipoprotein A1 infusions and cardiovascular outcomes after acute myocardial infarction. *N Engl J Med*. 2024;390:1560–1571.

**47.** Povsic TJ, Korjian S, Bahit MC, et al. Effect of CSL112 on recurrent myocardial infarction and cardiovascular death: insights from the AEGIS-II trial. *J Am Coll Cardiol*. 2024;83(22):2163–2174.

**KEY WORDS** cholesterol, familial hypercholesterolemia, HDL, LDL, macrophages, mice, PCSK9, reverse cholesterol transport

**APPENDIX** For supplemental figures and a table, and a dataset, please see the online version of this paper.